RSC Advances

ROYAL SOCIETY OF CHEMISTRY

www.rsc.org/advances

The Impacts of Various Operating Conditions on Submerged Membrane Photocatalytic Reactor (SMPR) for Organic Pollutant Separation and Degradation: A Review

C.S. Ong[a*], W.J. Lau[b*], P.S. Goh[b], B.C. Ng[b], A.F. Ismail[b], C.M. Choo[a]

[a]Faculty of Engineering and the Built Environment, SEGi University, 47810 Petaling Jaya, Selangor, Malaysia

[b]Advanced Membrane Technology Research Centre (AMTEC), Universiti Teknologi Malaysia, 81310 Skudai, Johor, Malaysia.

*Corresponding authors: Email address: ongchisiang@segi.edu.my (C.S. Ong), lwoeijye@utm.my (W.J. Lau)

Abstract

Rapid expansion and development of membrane based wastewater treatment in the recent decades have led to emerging technology - submerged membrane photocatalytic reactor (SMPR) that exhibit not only lower degree of fouling but also capable of separating and degrading organic pollutants simultaneously during treatment process. This review intends to provide an update on the influences of several key operational parameters, i.e. photocatalyst loading (both suspended and immobilized), feed pH and concentration, wavelength and intensity of UV light, membrane module packing density and air bubble flow rate on the efficiencies of SMPR in treating degradable organic pollutants. The structure and properties the photocatalytic membrane as well as the membrane performance stability under UV irradiation were also discussed. Understanding the effect of each operational parameter is of paramount important towards achieving optimum SMPR performance and addressing challenges encountered in the development of SMPR. Strategies and approaches are also recommended in this review in order to overcome the persistent problems and facilitate the research and development of SMPR.

Keywords: submerged membrane photocatalytic reactor, air bubble flow rate, pH, feed concentration, catalyst loading, light wavelength

1.0 Introduction

Water scarcity has been increasingly recognised as a serious and growing concern where deteriorating quality and growing demand for clean water sources have created significant challenge around the world. This issue has been further exacerbated by the rapid population growth, industrialization and booming of commercial activities that demand high volumetric of clean water resources. According to the World Health Organization (WHO), there are around 750 million people around the world who do not have access to an improved source of drinking water [1]. In view of this, numerous attempts have been undertaken for water and wastewater treatment in order to provide access to clean and safe water. With their outstanding attributes, photocatalytic membrane reactor (PMR) is highly considered as an alternative for water and wastewater treatment. In brief, PMR is a hybrid system that couples photocatalysis and a membrane process in one unit, as illustrated in Figure 1. The photocatalysis process allows the organic pollutants to be decomposed and mineralized to simple substances such as water (H_2O), carbon dioxide (CO_2) and mineral salts meanwhile the membrane enables the separation of photocatalyst from the reaction medium for further reuse. Additionally, the membrane could serve as a barrier for the initial compounds and by-products formed during decomposition, preventing them to pass through to permeate side.

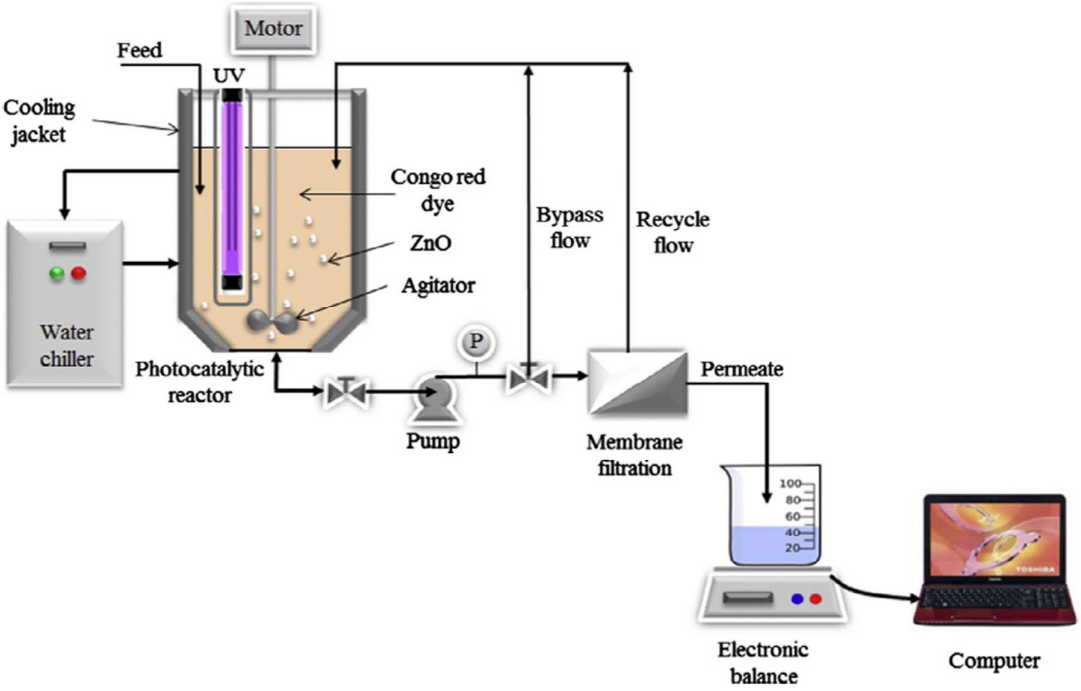

Figure 1: Schematic diagram of a laboratory-scale PMR with zinc oxide (ZnO) photocatalysts in suspension[2].

There are numerous configurations of PMRs being pursued by researchers. These include pressurized and depressurized (submerged) systems working in either batch or continuous mode. The pressurized PMR system can achieve higher flux compared to submerged system due to the higher driving force applied to the system. However, the major drawbacks of pressurized PMR system are the decline of permeation rate as a function of filtration time coupled with higher degree of surface fouling caused by remaining pollutants and/or suspended catalysts in the feed solution. The impact of suspended catalysts on membrane flux has been previously investigated by several research groups and their results have shown that suspended nanoparticles in the PMR system have negative effect on membrane permeability [3-5]. In this regards, the depressurized PMR system, also known as submerged membrane photocatalytic reactor (SMPR), has been generally agreed as alternative approach to overcome the problems encountered by pressurized system. Compared to pressurized conventional PMR, the most notable advantages of SMPR are its (1) possibility of operating at high flux with relatively low energy consumption and fouling tendency and (2) enhanced mass transfer between the UV light and targeted pollutants (for greater photodegradation efficiency) owing to the generation of air bubbles in the system [1].

In PMRs, the catalyst can be either immobilized on/in a membrane or suspended in the reaction mixture. Two main configurations for PMR are generally pursued, namely i) reactor with catalysts suspended in the feed solution and ii) reactor with catalysts immobilized in/on the membrane. The advantages and disadvantages of suspended and immobilized titanium dioxide (TiO_2) catalysts are summarized in Table 1. Although a suspended system offers a more intensive treatment, it requires additional process to separate catalysts from the suspended reactor. Many methods have been proposed to improve the recovery of the suspended catalysts. Some of them are 1) improving the catalysts aggregation through pH adjustment and 2) enhancing the separation of magnetic catalysts in a magnetic field. Nevertheless, these methods were only able to enhance the sedimentation and facilitate the recovery of catalyst in batch system [6-9].

Table 1: Comparison between TiO_2 suspended and immobilized reactor

TiO_2 suspended reactor	**TiO_2 immobilized reactor**
Advantages	**Advantages**
1. Higher photocatalytic area to reactor volume ratio 2. Higher mass transfer and degradation efficiency 3. Fairly uniform catalysts distribution 4. Adjustable amount of nanoparticle suspension in the reactor to deal with different compositions of treated solution	1. No separation and recycle of the catalyst 2. Less membrane fouling due to enhanced hydrophilicity of membrane surface upon nanoparticle incorporation 3. Pollutants could be degraded either in feed or in permeate
Disadvantages	**Disadvantages**
1. Higher operating cost and requires additional treatment after degradation process	1. Degradation efficiency is lower than that of suspension mode 2. Impossible to adjust the catalyst loading to deal with different compositions of treated solution 3. Replacement of membrane is required when catalyst loses its activity

Membrane photocatalytic reactor has attracted considerable attention among membrane scientists mainly due to its powerful and efficient capability for degrading and mineralizing recalcitrant compounds under vacuum pressure condition. This great achievement was initiated by Molinari in year 2002 [10] and presently SMPR has been extensively applied for the purification and disinfection of contaminated groundwater, surface water, and wastewater containing recalcitrant, inhibitory, and toxic compounds with low biodegradability.

Comprehensive overview and detailed discussion on the development of PMR have been previously published in several review articles[11-13]. A broad range of subject matters such as fundamental mechanism, reactor configurations, operational parameters, kinetics and modelling, the water quality analysis as well as the related life cycle assessment have also been covered, but mainly focused on the development between 1990 and 2010. Also, brief description on the types of photocatalytic membranes, PMR configuration and potential applications could be found in several recently published book chapters [14-17]. However, the rapid expansion and increasing demand of employing SMPR in water and wastewater

treatment over the past several years have motivated us to provide an update on the recent progresses of SMPR applications. The most significant contribution of this review is to highlight and emphasize the importance of operating conditions on the performance of SMPR followed by discussion on the existing challenges and strategies that can be implemented to heighten the current performance of SMPR.

2.0 Factors Affecting the SMPR Performance

In this section, a brief review on the performance of SMPR with different operating parameters for water and wastewater treatment is presented. The influences of various operating parameters on the photodegradation efficiency and membrane separation performance of SMPR are highlighted. Several operating parameters such as catalyst loading, UV light wavelength and its intensity, feed concentration and pH, module packing density, air bubble flow rate (ABFR), are discussed. Table 2 summarizes several important findings on the SMPRs that were previously reported for treating different types of organic pollutants. The photocatalytic activities of the system are found to be closely associated with operating parameters as mentioned before. Thus, it is of great significance to study the correlation between these parameters in order to fully understand their impacts on the SMPR performance.

2.1 Catalyst Loading

Catalyst loading is a one of the key operating parameters which could affect the photocatalytic oxidation rate. The amount of photocatalyst used in the process is directly proportional to the reaction rate [11]. The principal mechanism of photocatalytic degradation is described as follows. When a photocatalytic surface is exposed by a radiation of energy equal to or greater than the bandgap energy, it will create a positively charged hole in the valance band and negatively charged electron in the conduction band by exciting the electrons in the valance band to the conduction band. The conduction band electron reduces oxygen into O_2^- which can be adsorbed by photocatalyst surface whereas the positively charged hole oxidizes either organic pollutants directly or indirectly by water to produce hydroxyl free radicals (HO·). These generated species act as powerful oxidizer to disintegrate harmful organic pollutants in wastewater and convert them into CO_2 and H_2O. When the photocatalyst loading is increased, there is an increase in the number of active surface sites available for adsorption and degradation. However, exessive use of photocatalyst would increase the solution opacity (for photocatalyst suspension case), reducing UV light penetration in the reactor [18-20].

Moreover, the loss in the surface area by catalyst agglomeration at high photocatalyst loading (for both catalyst suspension and immobilization case) is likely to cause the UV light scattering and deteriorate the overall photocatalytic performance [21-23]. Therefore, any chosen photoreactor should be operated below the saturation level of photocatalyst in order to ensure efficient photons absorption. With respect to the membrane flux performance, it is generally reported that an increase of photocatalyst loading tends to negatively affect permeate flux, mainly because of the catalyst agglomeration on the membrane surface which creates additional transport resistance to water molecules[15,24].

Table 2: The influences of various SMPR operating conditions on photodegradation performances in SMPR system

Type of photocatalyst/Max loading	[a]Membrane configuration/ Polymer	Operating conditions	System/ Reactor volume	[b]Targeted pollutant(s)	Initial concentration/ Range of concentration	Type of UV/Power intensity	Time required to degrade at least 50% of pollutants (h)	Ref.
Degussa P25 TiO_2/ 0.5 g/L	Flat sheet/ PTFE	Submerged membrane with TiO_2 catalyst suspension ABFR: 1.5 L/min, pH 6.4-6.9	3 L	RB5 dye	125 ppm	UVC (15 W, intensity: N/A)	~120 min (with 0.5 g/L TiO_2 at 100 ppm)	Damodar et al. [25]
Degussa P25 TiO_2/ 1 g/L	Hollow fiber/ N/A	Submerged membrane with TiO_2 catalyst suspension. ABFR: null; Pohang seawater: pH 8.1; Masan seawater: pH 8.2 Mooncheon lakewater: pH 7.98	800 mL	Two seawater sources (from city of Pohang and city of masan) and Mooncheon lakewater	Pohang seawater: 0.198 ppm (TOC), Masan seawater: 2.03 ppm (TOC) Mooncheon lakewater: 4.91 ppm (TOC)	UVA (8 W, intensity: N/A)	Mooncheon lakewater: ~90 min (with 1 g/L TiO_2 at 4.91 ppm); No significant TOC reduction for Pohang and Masan seawater	Kim et al. [26]
Degussa P25 TiO_2/ 0.6 g/L	Hollow fiber/ polypylene (PP) or PVDF	Submerged membrane with TiO_2 catalyst suspension. ABFR: 5 L/min, pH: N/A	4 L	HA	TOC: 10 ppm	UVA (8 W, intensity: N/A)	~15 min (with 0.6 g/L TiO_2 at 10 ppm)	Halim et al. [27]
Degussa P25 TiO_2/ 0.5 g/L	Flat sheet/ PVDF	Flat submerged membrane with TiO_2 suspension. ABFR: 4 L/min, pH 7	8 L	HA	DOC: 10 ppm	UVC (16 W, 1.17 mW/cm^2)	~30 min (with 0.5 g/L TiO_2 at 10 ppm)	Yong et al. [28]
Degussa P25 TiO_2/ 1.5 g/L	Hollow fiber/ PVDF	Submerged membrane with TiO_2 catalyst suspension. ABFR: 20 L/min, pH: N/A	9 L	Polysaccharides	TOC: 2.5 ppm	Three UV-A (30 W, 8.3 mW/cm^2)	< 360 min (with 0.5 g/L TiO_2 at 2.09 ppm)	Sarasidis et al. [29]
Degussa P25 TiO_2/ 1 g/L	Hollow fiber/ PVDF	Submerged hollow fiber membrane with P25 TiO_2 suspension, pH: N/A	1 L	Carbamazepin (CBZ)	5 ppm	240 units of vis-LED (<0.5 W/m^2)	~120 min (with 1 g/L TiO_2 at 5 ppm)	Wang et al. [30]

Table 2: (*Continue....*)

Type of photocatalyst/Max loading	Membrane configuration/ Polymer	Operating conditions	System/ Reactor volume	Targeted pollutant(s)	Initial concentration/ Range of concentration	Type of UV/Power intensity	Time required to degrade at least 50% of pollutants (h)	Ref.
Degussa P25 TiO_2/ 18 wt.%	Hollow fiber/ Polyethylenimine (PEI)	Submerged membrane embedded with TiO_2 catalyst; ABFR and pH: N/A	25 ml	Acid orange 7 (AO7)	20 ppm	Four UVA (8 W, intensity: N/A)	< 60 min (with 18 wt.% TiO_2 at 20 ppm)	Zhang et al. [31]
Degussa P25 TiO_2/ 0.75 g/L	Hollow fiber/PVDF	Submerged membrane with TiO_2 catalyst suspension ABFR: 5L/min, pH 6.8	3 L	Dichlofenac (DFC)	2.5 ppm	Four UVA (24 W, 14.4 mW/cm^2)	<300 min (with 0.5 g/L TiO_2 at 2.5 ppm)	Sarasidis et al. [23]
Degussa P25 TiO_2/ 0.5 g/L	Hollow fiber/ PVDF	Submerged membrane with TiO_2 catalyst suspension ABFR: 1.2 L/min, pH 3, 8	4 L	Trace organic compound (TrOC)	0.5 ppm	Seven UVA (8 W, intensity: N/A)	< 240 min (with 0.5 g/L TiO_2 at 0.5 ppm)	Fernandez et al. [32]
Anatase TiO_2/ 2.0 g/L	Hollow fiber/ polypropylene (PP)	Submerged membrane with TiO_2 catalyst suspension ABFR: 3 L/min, pH 3, 7 and 10	5 L	Acid Red 1 azo dye (AR1)	15-75 ppm	UVC (8 W, 62.91 mW/cm^2)	~80min (with 0.5 g/L TiO_2 at 15 ppm)	Kertesz et al. [33]
Degussa P25 TiO_2/ 4 wt%	Hollow fiber/ PVDF	Submerged membrane embedded with TiO_2 catalyst ABFR: 1-5 L/min, pH 7	14 L	Oil molecules	250 - 10,000 ppm	UVA (8 W/0.333 mW/cm^2)	~60 min (with 2 wt% TiO_2 at 1000 ppm)	Ong et al. [34]
TiO_2-ZrO_2/ 0.15 g/L	Hollow fiber/ PVDF	Submerged membrane with TiO_2 catalyst suspension. ABFR: 4 L/min, pH 4	2 L	HA	50 ppm	UVC (4 W, intensity: N/A)	<240 min (with 0.15 g/L TiO_2-ZrO_2 at 50ppm)	Khan et al. [35]

[a] PTFE - Polytetrafluoroethylene, PVDF – Polyvinylidene Fluoride, PEI – Polyethylenimine and PP - Polypropylene

[b] RB5 – Reactive Black 5, HA – Humic Acid, CBZ – Carbamazepine, AO7 – Acid Orange 7, DFC - Dichlofenac, TrOC – Trace Organic Compound, AR1 – Acid Red 1 azo dye

Furthermore, the performance of SMPR at optimum catalyst loading can also be influenced by the dimension of the photoreactor. It is because different reactor designs tend to have different water flow hydrodynamics and photons absorption rate [11]. Large reactor volume usually have lower saturated catalyst loading and lower efficiency compared to small reactor. A considerable amount of studies have reported the effect of TiO_2 loadings on the process efficiency, as summarized in Table 3 [18-21]. The observed discrepancies in photodegradation and membrane performance can be attributed to differences in the reactor configurations, light sources and contaminants properties as well as the interaction between operating conditions employed. In order to avoid an excessive use of the photocatalysts and to ensure the highest efficiency of photodegradation, it is very important to determine the optimum catalyst loading based on the characteristics of wastewater.

Table 3: Effect of TiO_2 catalysts loadings on the SMPR photodegradation performance

Targeted pollutant	Photocatalyst	Range of catalyst loadings	Optimum catalyst loading	Light source, power and intensity	Ref.
Fulvic Acid	Suspended	0-0.6 g/L	0.5 g/L	UVC 11W, 0.75 mW/cm^2	18
Bisphenol-A	Suspended	0.2-2 g/L	0.5 g/L	UVA 8W, intensity: *N/A*	19
Biologically treated sewage effluent	Suspended	0.5-1.0 g/L	1 g/L	UVA 10W, 46.15-276.96 mW/cm^2	21
Polysaccharide	Suspended	0.25-1.5 g/L	0.5 g/L	Three UV-A 30W, 8.3 mW/cm^2	23
Acid Red 1	Suspended	0.01-2 g/L	0.5 g/L	UVC 8W, 62.91 mW/cm^2	33
Oily wastewater	Immobilized	0-4 wt.%	2 wt%	UVA 8W, 0.333 mW/cm^2	34
Carbamazepine	Suspended	0.3-1 g/L	1 g/L	240 units of vis-LED with intensity <0.5 W/m^2	30

2.2 Feed Concentration

As reported in the literature, the degradation rate of targeted pollutants is mainly influenced by the initial concentration of the pollutants. The Langmuir-Hinshelwood model as expressed in Equation (1) describes the relationship between organic compound concentration and its photodegradation rate

$$r = -\frac{dC}{dt} = \frac{k_r K_{ad} C}{1 + K_{ad} C} \quad (1)$$

where k_r is the intrinsic rate constant (mg/L.min) and K_{ad} is the adsorption equilibrium constant (L/mg). When the adsorption is relatively weak and/or the concentration of organic compound is low, Equation (1) can be simplified to the first-order kinetics with an apparent rate constant k_{app} (min^{-1}) as shown in Equation (2).

$$\ln\left(\frac{C}{C_0}\right) = -k_r K_{ad} t = -k_{app} t \quad (2)$$

C_0 is the initial concentration of organic pollutant (mg/L), C is the final concentration of the pollutant after time t of the photocatalytic decomposition (mg/L), k_{app} is the apparent rate constant of a pseudo first order reaction (min^{-1}) and t is the time of photocatalysis (min). According to Equation (2), the reaction rate is expected to increase with irradiation time due to the decreasing amount of contaminants [11].

Table 4 summarizes the findings from the previous works on the feed concentration study in which optimum PMR performance can be achieved. According to Kertesz et al. [33], as dye concentration increases, the color of the irradiated solution becomes more intensive and concentrated, which in turn affects the penetration depth of UV light. The dye molecules also tend to absorb part of the light photons (UV-screening effect of the dye itself), leading to insufficient photon energy for hydroxyl radical generation[33, 36]. Furthermore, the thick fouling layer formed at high feed concentration would adversely affect photocatalytic degradation due to lesser active surface sites for UV irradiation. This is further supported by a recent work where the degradation of oil under UV irradiation was highly efficient at low concentrations (see Figure 2) [24].

In the contrary, Halim et al. [27] reported that photocatalytic efficiency increased with the increasing initial total organic carbon (TOC) concentration of HA from 5 to 50 ppm, owing to the larger amount of reactants anticipated in the reaction mixture that led to more frequent collisions between the organic molecules and the catalyst particles and higher

adsorption rate. As implied in the abovementioned studies, PMR membrane achieves optimum performance depending on the characteristics of targeted pollutants.

Table 4: Effect of feed concentration on the photodegradation performance of SMPR that used TiO_2 as photocatalyst

Targeted pollutants	Range of feed concentration (ppm)	Feed concentration in which optimum performance achieved (ppm)	Light source, power and intensity	Ref.
Bisphenol-A	10-50	10	Four UVA 8W, intensity: N/A	37
Humic acid	1-10	1	UVA 8W, intensity: N/A	38
Biologically treated sewage effluent	0-100	50	UVA 10W, 46.15-276.96 mW/cm^2	21
Acid Red 1	15-75	15	UVC 8W, 62.91mW/cm^2	33
Synthetic oily wastewater	250-10000	250	UVA 8W, 0.333 mW/cm^2	34
Carbamazepine with humic acid	[a]1.5-14.5	5	240 units of vis-LED 15-60 W, <0.5 W/m^2	30
Humic acid	[a]5-50	10	UVA 8W, intensity: N/A	27

[a]The concentration of the organic components was determined based on total organic carbon (TOC)

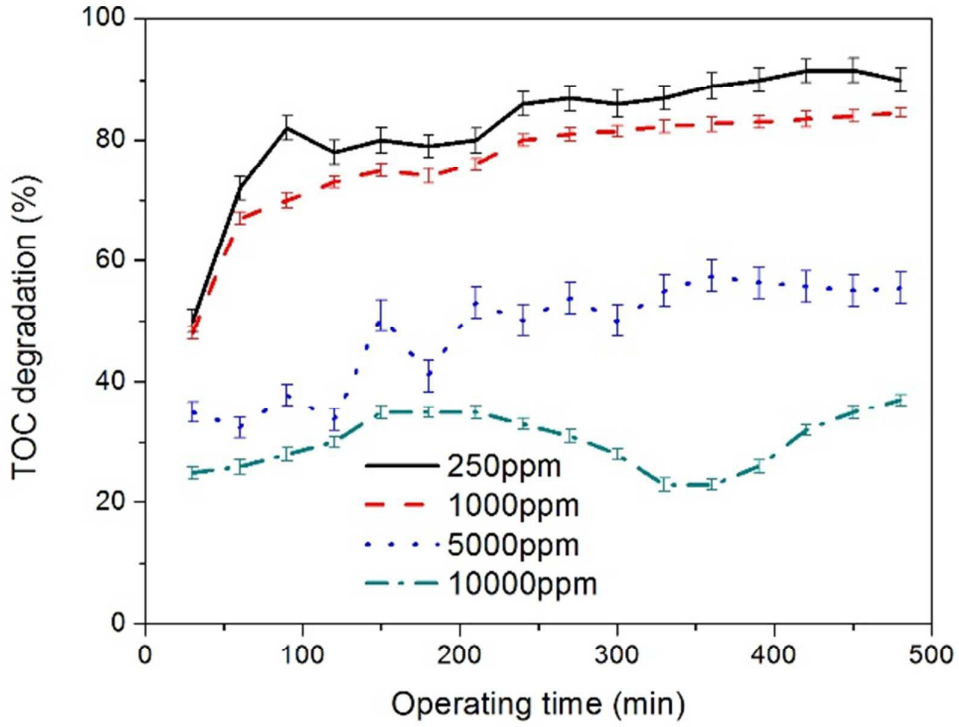

Figure 2: Effect of feed concentration on TOC degradation of PVDF-TiO_2 composite membrane in the SMPR system (Operating conditions: temperature = 25 °C, membrane type: PVDF with 2 wt.% TiO_2, module packing density = 35.3%, vacuum pump flow rate = 15 mL/min and pH = 7) [24]

2.3 Module Packing Density

Very few studies were devoted to investigate the impacts of module packing density on the permeate flux. The voids among the fibers not only act as water flowing pathway but also facilitate mass transfer between the feed and membrane surface [39-43]. Although high packing density of small diameter hollow fibers can contribute to high filtration surface area, it at the same time promotes severe inter-fiber fouling due to the unfavorable hydrodynamic conditions within the fibers [44, 45].

One recent work has reported that permeate flux increased with increasing module packing density from 17.6% to 35.3%, owing to the enhanced mass transfer between the water molecules and membrane surface (see Figure 3). However, when the module packing density was further increased to 52.9%, the fibers were likely to attach to each other and resulted in the limited spaces available between adjacent fibers, hence reduced the active surface sites for UV irradiation. This as a consequence, deteriorated both photodegradation

and membrane flux. This is in agreement with the experimental work conducted by Kiat et al. [46] where severe fouling tended to occur when the packing density of the module exceeded a critical value, i.e. 30.8%. Under optimized packing density, Yeo et al. [41] reported that promising membrane permeability could be achieved. However, it must be pointed out that high density of fiber packing could cause foulant accumulation inside the fiber bundle and adversely decrease the permeability. Contradictory results were reported by Gunther et al. [44] where the water flux increased by 25% when the fiber packing density was decreased from 80% to 40%. This enhancement was attributed to the suppression of cake layer formation when low packing density of hollow fiber membranes were used.

Wu and Chen [47] investigated the effect of flow distribution on shell-side mass transfer performance in randomly packed hollow fiber modules. They observed that the mass transfer coefficient was rapidly decreased with increasing packing density until 50% of total volume fraction, and further increased the packing density tended to increase the mass transfer coefficient. They attributed the improved mass transfer coefficient to the better orientation of hollow fibers which facilitated the water flowing through the adjacent fibers. As can be seen, the optimum packing density varies depending on the feed solution properties, module dimension and membrane material. Extensive work on this subject is certainly needed to provide a better understanding on how the module packing density governs the efficiency of photodegradation.

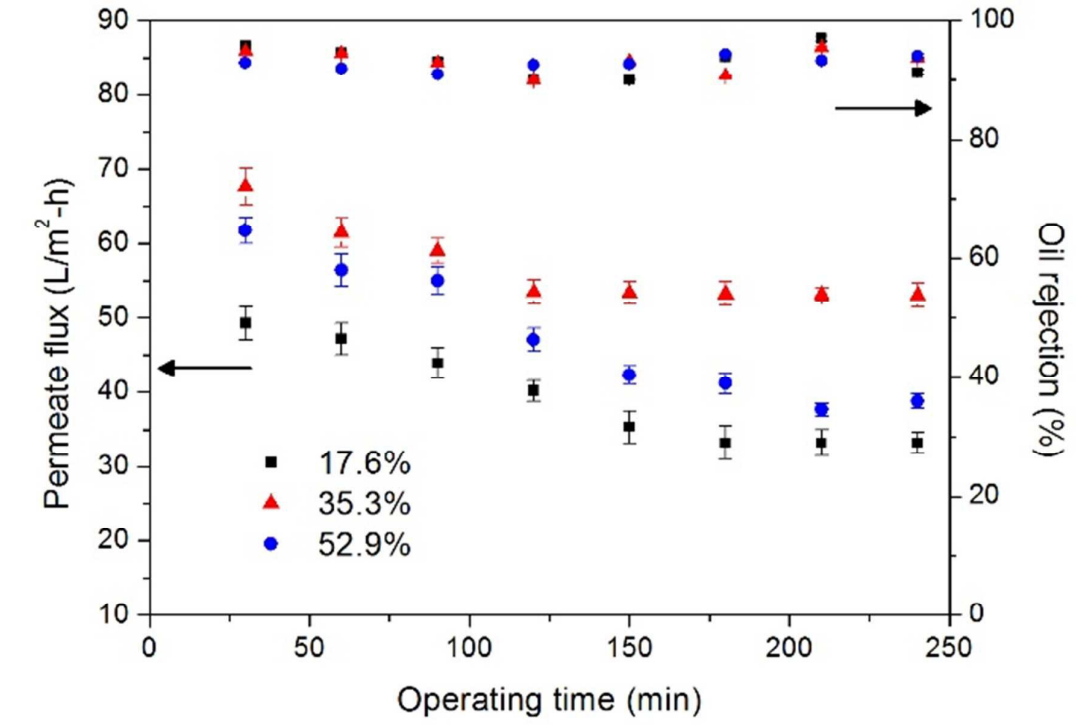

(a)

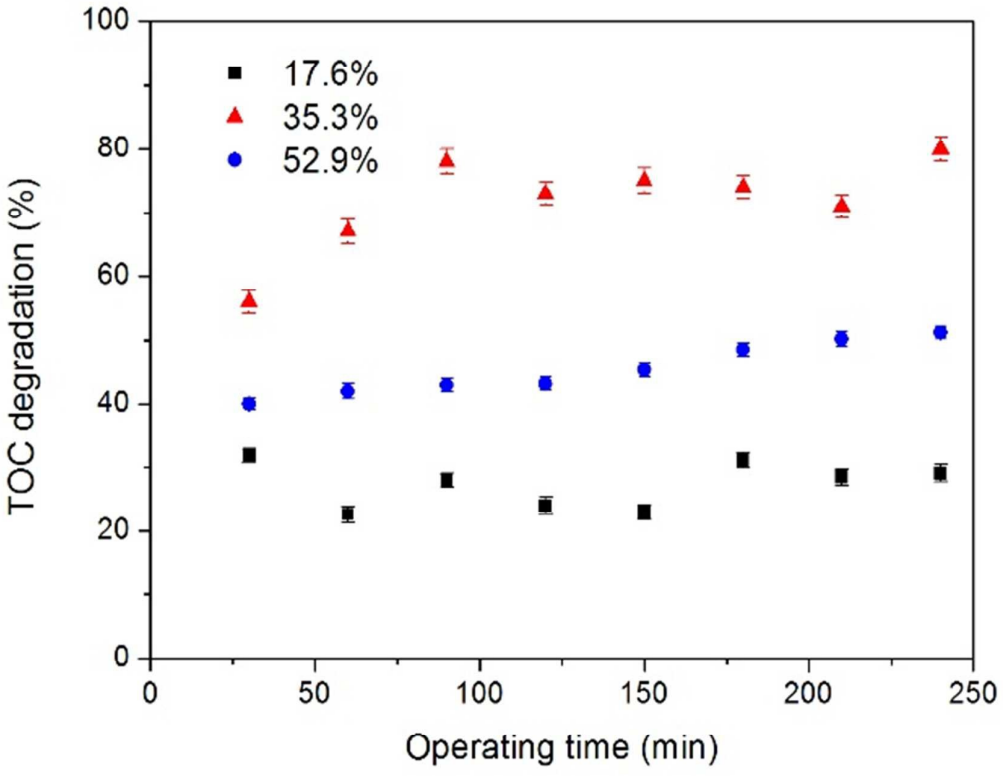

(b)

Figure 3: Effect of module packing density on (a) permeate flux and oil rejection and (b) TOC degradation of PVDF-TiO_2 composite membrane in the SMPR system (Operating conditions: temperature = 25 °C, membrane type: PVDF with 2 wt.% TiO_2, vacuum pump flow rate = 15 mL/min and pH = 7) [24]

2.4 Air Bubble Flow Rate (ABFR)

Air bubble flow is able to alleviate the fouling problem based on the generation of circulation flow that enhances the mixing of pollutants and restricts their attachment on the membrane surface. When air bubbling scours the membrane surface, it can detach the deposited cake layer on the membrane surface and thus increase membrane water flux. With respect to photocatalytic activity, higher photocatalytic degradation can be achieved when higher ABFR is applied in the SMPR system. Briefly, the detailed mechanism can be explained by the following pathways. OH· radicals are generated from an abundant of oxygen bubbles as a result of higher ABFR (Eq. 3 & 4) and also from the dissociation of water molecules upon UV illumination (Eq. 5). These OH· radicals mineralize the hydrocarbon groups in the organic-based wastewater to become CO_2 and H_2O (Eq. 6). Figure 4 illustrates the mechanism of photocatalytic reaction in the presence of air bubbles.

With air flow (O_2 ~ 78 %) under 365 nm irradiation [48]:

$$\text{Oxygen bubbles} \xrightarrow{h\nu} \text{Dissolved oxygen} \xrightarrow{h\nu} \text{Ozone } (O_3) \quad (3)$$

$$\text{Ozone } (O_3) \longrightarrow O\,(^1D) + H_2O \longrightarrow 2\,OH\cdot \quad (4)$$

(formation of hydroxyl radicals)

$$H_2O \xrightarrow{h\nu} H\cdot + OH\cdot \quad (5)$$

$$\text{Oil} + 3\,OH\cdot \longrightarrow xCO_2 + yH_2O \text{ (mineralization)} \quad (6)$$

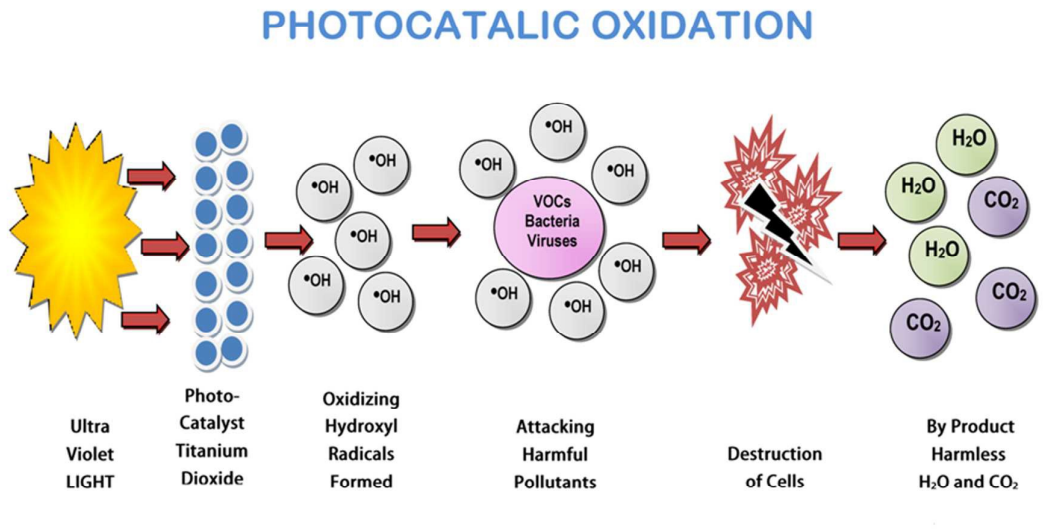

Figure 4: The schematic diagram of photocatalytic reaction with the presence of air bubbles [49]

The ABFR plays an important role in photocatalytic reaction since the supplied oxygen could provide sufficient electron scavengers to trap the excited conduction band electron from recombination [11]. The flux improvement at higher ABFR is likely due to the generation of circulation flow in the SMPR which limits the adsorption of pollutants onto the membrane surface and further reduces the membrane fouling tendency. The large airflow might enhance the mass transfer inside the treated wastewater and more OH^- radicals would be produced in the feed solution, which in turn results in higher photodegradation efficiency and membrane water flux. However, when excessive air bubbles present in the system, the adsorption reaction of targeted pollutants onto the suspended catalyst will be greatly reduced, which may result in lower degradation rate since photocatalytic oxidation is a surface-oriented reaction. Chin et al. [19] investigated the degradation of TiO_2 suspended submerged membrane reactor by varying ABFR from 0.2 to 4 L/min. The photocatalytic reaction rate increased with an increase in bubbling rate and reached a maximum value at a bubbling rate of 0.5 L/min. Bubbling can increase the liquid film mass transfer coefficient around the aggregates but it may also provide a bubble cloud that can attenuate UV light transmission in a photoreactor. The balance of the competing effects between mass transfer and light attenuation might lead to an optimal bubbling rate which can achieve highest photodegradation efficiency [30].

2.5 Feed pH

In SMPR, initial pH of the solution is of importance as it dictates the surface charge properties of the particles, affecting the sorption of targeted compounds on the catalyst surface. Many studies have discovered that pH would affect the interaction between targeted compounds and membrane surface. As mentioned in a review article published in 2010 [12], the effect of pH on photodegradation of organic pollutants is associated with (1) the ionization state of photocatalyst surface, (2) position of the valence and conduction bands of the photocatalyst, (3) agglomeration of photocatalyst particles and (4) formation of hydroxyl radicals. Wang et al. [30] performed a work to investigate the degradation of CBZ at different pH using synthesized C-N-S tridoped TiO_2 nanoparticles. Their experimental results indicated that higher CBZ degradation rate could be achieved at alkaline condition as compared to that of acidic region. This was attributed to the formation of more OH· radicals at higher pH, leading to higher CBZ photocatalytic degradation. It is commonly found that in alkaline solution, OH· can be generated more easily by oxidizing more hydroxide ions on TiO_2 surface [19, 30, 50]. Figure 5 illustrates how the presence of OH- ions could improve the efficiency of the process.

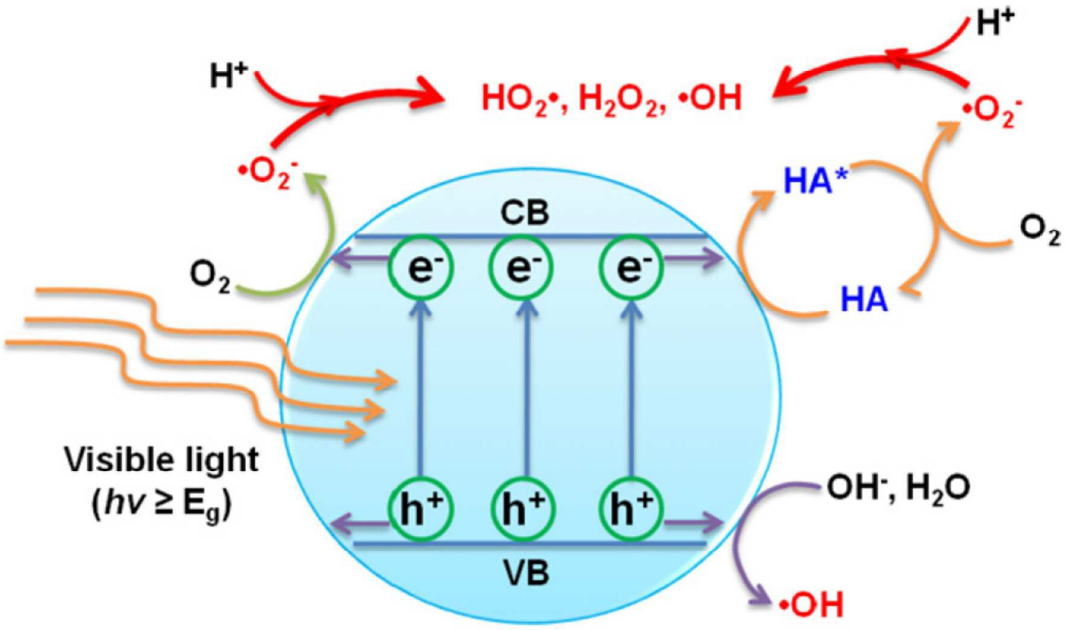

Figure 5: Proposed mechanism of CBZ degradation with HA in the TiO_2 suspension under vis-LED irradiation [30]

It is worth mentioning that the concentration of OH· might increase with the increasing concentration of H^+ in the acidic condition [18, 51, 52]. This is in agreement with the work conducted by Chin et al. [37] where BPA degradation at low pH was remarkably higher than that of high pH. As the pH was increased, the TiO_2 surface became progressively more negative and led to the development of greater repulsive forces between the TiO_2 surface and BPA compounds, thus retarded the total degradation efficiency. Similarly, Khan et al. [53] found that HA degradation was two times higher at low pH compared to that obtained at high pH (see Figure 6). This is most likely due to the stronger electrostatic attractions between the HA and photocatalyst TiO_2–ZrO_2 at acidic environment. Table 5 summarizes the effects of pH on the photodegradation of various pollutants using SMPR treatment process. It is revealed that organic molecules tend to have different photocatalytic reactivities at different pH environment, depending on the nature of respective pollutants.

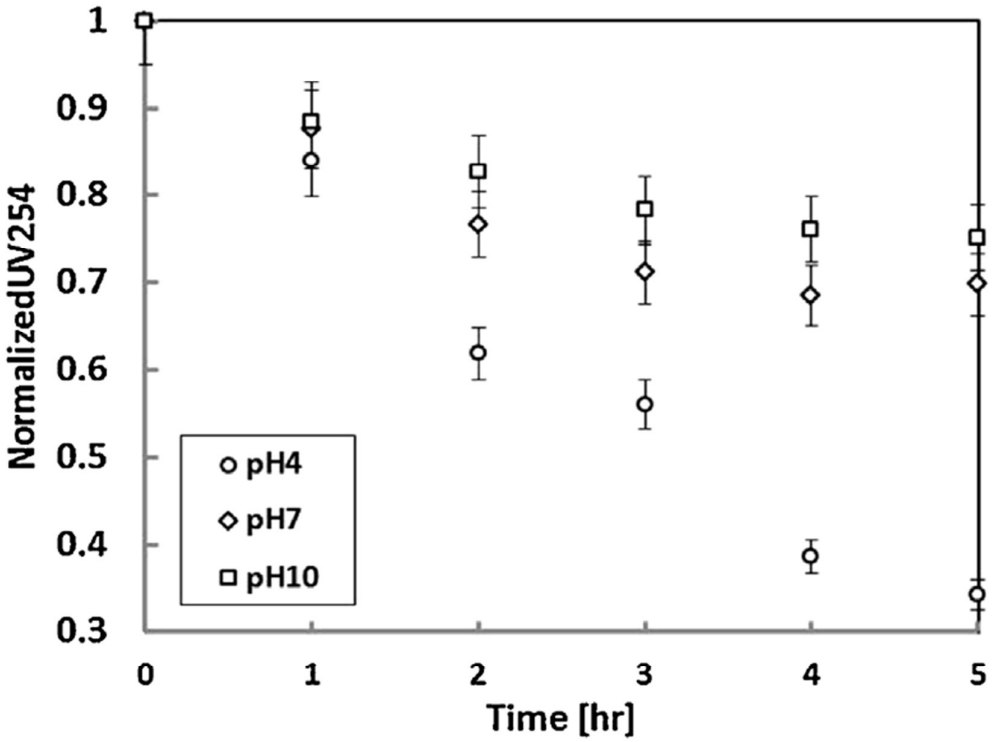

Figure 6: Effects of pH solution on UV_{254} removal efficiency [HA] = 50 mg/L, temperature = 28°C using TiO_2–ZrO_2 particles [53]

Table 5: Influence of pH on the photocatalytic degradation of PMR using TiO_2 as photocatalyst

Targeted pollutants	Tested pH value	Optimum pH	Light source and its intensity	Ref.
FA	3.4, 6.5, 8.2 and 10.3	3.4	UVC 11W, 0.75 mW/cm^2	18
BPA	4, 7 and 10	4	UVA 8W, intensity: *N/A*	37
AR1	3, 7 and 11	11	UVC 8W, 62.91 mW/cm^2	33
HA	4, 7 and 10	4	UVC 4W, intensity*: N/A*	53
CBZ	3, 6, 9 and 12	12	240 units of visible LED with intensity <0.5 W/m^2	30

2.6 Light Wavelength and Intensity

UV wavelength has significant effect on the photocatalytic reactivity. For UV irradiation, its corresponding electromagnetic spectrum can be classified into UV-A (315-400 nm) (3.10-3.94 eV), UV-B (280-315 nm) (3.94-4.43 eV) and UV-C (100-280 nm) (4.43-12.4 eV) [11]. According to a study, only 5% of the total irradiated natural sunlight has sufficient energy to initiate effective photodegradation [54]. The need for continuous illumination for efficient photocatalytic process has diverted solar utilization to artificial UV lamp-driven process.

In particular, light intensity is one of the few parameters that affects the degree of photocatalytic reaction on organic substrates. A relatively abundant light intensity is required to adequately provide the catalyst surface active sites with sufficient photons energy. The photoactivity of catalysts in the presence of UV wavelength (< 400 nm) in many studies obeys the linear proportional correlation to the incident radiant flux and becomes steady at excessive radiant flux in the photoreactor. This phenomenon is observed by Ho and his co-workers [21] where the organic matters from biologically treated sewage effluent (BTSE) was treated by SMPR system. As shown in Figure 7, similar tendency of photocatalytic degradation was observed irrespective of light intensity that was degradation rate dropped signficantly for the first 30 min of operation followed by almost constant rate when all particles absorbed photons and produced electron-hole pairs. Considering the energy consumption, the minimum intensity of 46.61 mW/cm^2 was determined as the optimum intensity.

Recently, Wang et al. [30] also reported the enhancement of CBZ photocatalytic degradation efficiency with the increasing visible-light intensity. Compared to 68% removal of CBZ under high intensity UV irradiation, only 28% of CBZ was able to degrade at low intensity UV irradiation. Furthermore, Kertesz et al. [33] compared the decolorization of the aqueous acid red 1 (AR1) solution under two different UV light wavelengths (254 nm and 366 nm). As can be seen from Figure 8, no decolorization of the aqueous AR1 solution occurred in the absence of catalyst using lower UV wavelength. A complete decolorization of the AR1 could only be achieved with the simultaneous presence of catalyst and UV irradiation. A faster initial degradation was observed at 254 nm compared to 366 nm, but at the end of the irradiation experiments (at 90 min) the two decolorizations were nearly equal. Fujishima et al. [55] however indicated that the initiation of photocatalysis reaction rates is not highly dependent on light intensity as very few photons of energy can sufficiently induce the surface reaction. Based on the findings, it can be concluded that the impact of different operating parameters on PMR performacne is very complicated and an optimum condition for a specified application should be selected on the basis of several preliminary studies with similar operational parameters.

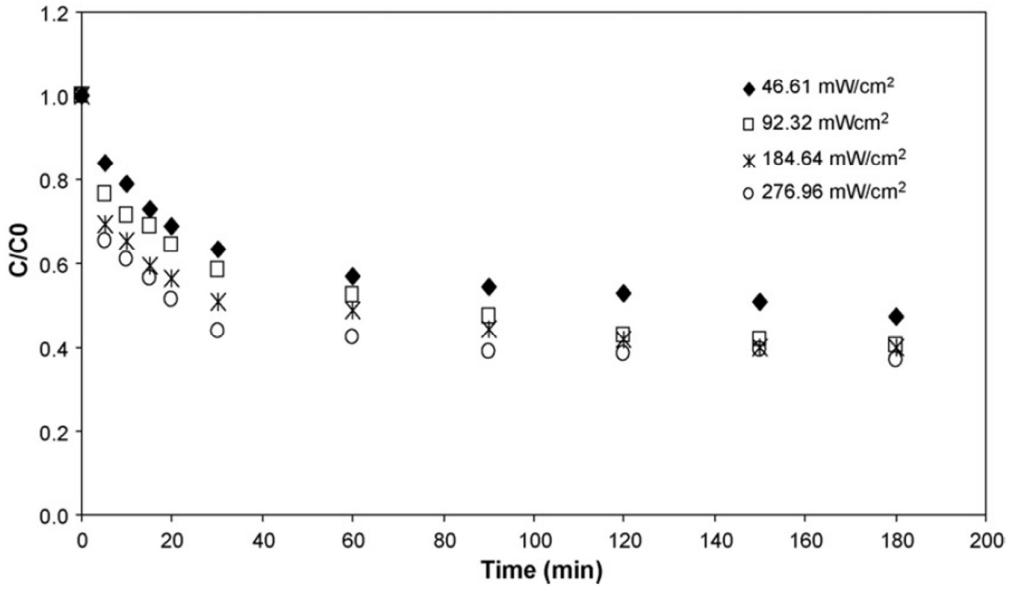

Figure 7: Effect of UV light intensity on the photooxidation process (Operating conditions: initial TOC = 12.47 mg/L; TiO_2 concentration = 1.0 g/L) [21]

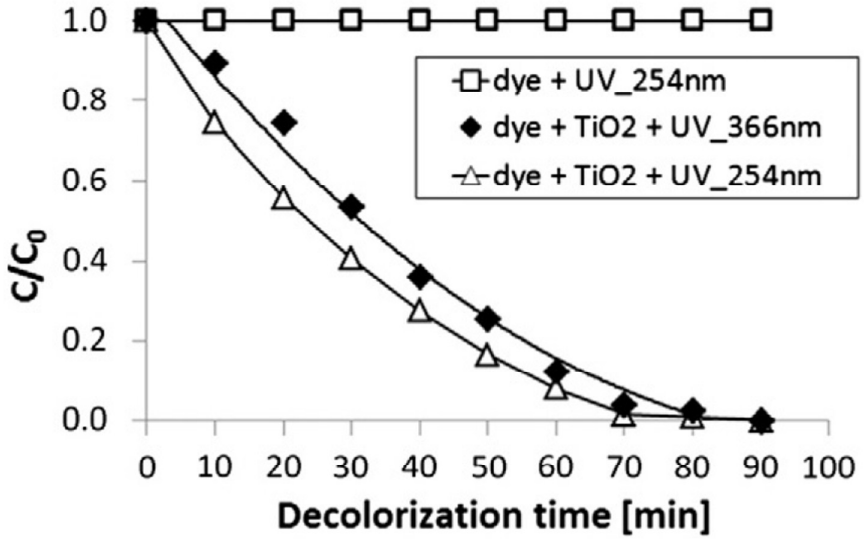

Figure 8: Influence of UV irradiation wavelength on the decolorization process (Operating conditions: C_0 = 15mg/L, C_{TiO2} = 0.5 g/L, pH=7, T = 25 °C, n = 400 rpm, I_{UV} = 62.9 mW/cm^2) [33]

2.7 Structure and Properties of Photocatalyst

Apart from the operating parameters, it is also important to understand the photoactivity of the selected catalysts that is dependent on surface and structural properties of photocatalytst such as crystal composition, surface area, particle size distribution, porosity and band gap energy[56]. Of these properties, band gap energy is the main criteria for a catalyt to be selected. Several works have compared the photocatalytic activities of different semiconductors in the process of degrading aqueous pollutants. For instances, Miyauchi et al.[57] studied the effect of different oxides (e.g. TiO_2, SnO_2, ZnO, WO_3, $SrTiO_3$, V_2O_5, CeO_2, CuO, MoO_3, Fe_2O_3, Cr_2O_3 and In_2O_3) on the degradation rate of methylene blue (MB) adsorbed on the thin film surface. Among them, TiO_2, $SrTiO_3$ and ZnO exhibited the highest photodegradation of MB under UV illumination followed by SnO_2 which showed relatively low photoactivity. The rest of oxides were found inactive for MB degradation. They attributed the results to the different band gap energy of photocatalysts as shown in Figure 9. When photocatalyst possesses higher band gap energy, more photon energy is required to promote the electron from valence band to conduction band, thus reduces the photodegradation efficiency. On the other hand, Khalil and his co-workers[58] evaluated the

efficiency of TiO_2, ZnO and WO_3 over the photodegradation of aqueous Cr(VI) and found that the photodegradation of Cr(VI) followed the pattern of TiO_2 > ZnO > WO_3. The findings were in agreement with the work of Miyauchi et al.[57]

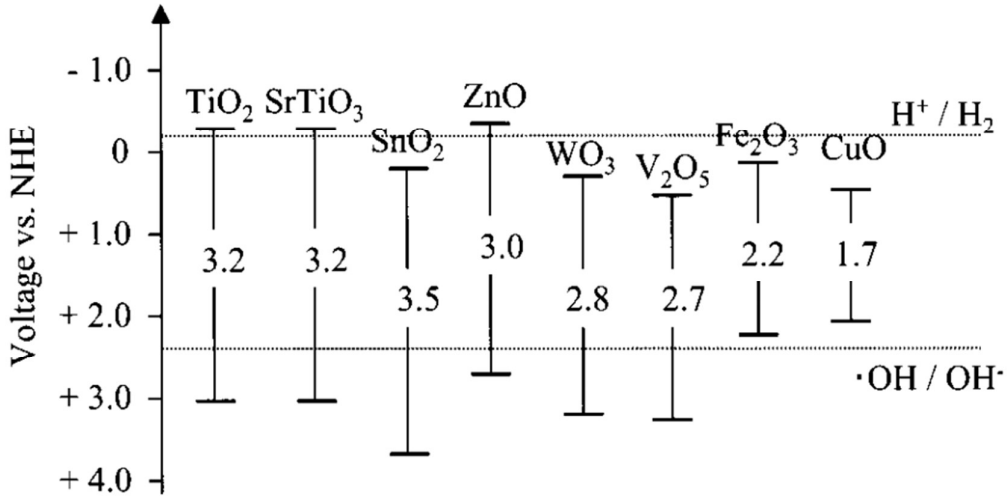

Figure 9: The redox potentials of valence and conduction bands as well as band-gap energies for various metal oxides at pH 7. The redox potential positions of H+/ H_2 and OH• /OH- at pH 7 are also illustrated (*NHE: Normal Hydrogen Electrode)[57]

Furthermore, Luisa et al.[59] compared the photodegradation efficiency of diphenhydramine (DP) and methylene orange (MO) by incorporating three different photocatalysts, i.e. self-synthesized TiO_2, graphene oxide combined with TiO_2 (GO-TiO_2) and commercial P25-TiO_2 into the flat sheet membrane. The results indicated that the membranes prepared with the GO-TiO_2 composite exhibited the highest photocatalytic activity, owing to the lowest band gap energy coupled with highest surface area compared to TiO_2 catalyst. The current research priority of catalyts development is focused on reducing the band gap energy of particles, in addition to greater surface area, aiming to achieve faster degradation rate.

2.8 Membrane Performance Stability

In general, there is a possible deterioration of membrane performance by formation of hydroxyl radicals and/or byproducts from partial degradation of pollutants under UV irradiation. The impact is greater particularly for the membranes made of polymeric materials. Mozia et al.[60] have previously evaluated the influence of process conditions and photocatalyst

type on the stability of four commercial ultrafiltration membranes made of polyethersulfone with respect to flux and dextran removal rate. They found that the effect of reactive oxygen species on the stability of membrane was not significant as compared to the photocatalyst particle itself (for suspension case). For photocatalyst suspension case, the membrane surface was possibly damaged by the suspended photocatalysts in the feed when large air flow was applied in the reactor. It was suggested that focus should be placed on the enhancement of membrane stability to the abrasion caused by the photocatalyst. Furthermore, the transmembrane pressure was found to have significant influence on the membrane stability. Cross flow velocity meanwhile has very little impact on membrane damage throughout the treatment process. Chin et al.[61] and Molinari et al.[62] also reported that suspended TiO_2 in the SMPR system has reduced the lifespan of the photocatalytic membrane. With respect to pH, Menderet et al. [63] showed that AO7 organic compounds were greatly absorbed on the membrane surface at acidic conditions due to the electrostatic attraction, causing a rapid fouling on the membrane surface and a reduced water flux.

3.0 Challenges in SMPR Development

The excitement and great benefits harnessed from the SMPR development have spurred great interest in wastewater industry sectors. To ensure the constant and steady development of these innovative and sustainable technologies, several key technical constraints ranging from photocatalytic membrane properties to process operating condition should be carefully addressed. The current photocatalytic membranes are still facing challenges where the contact area between photocatalyst, targeted pollutant and UV light is lower than in the catalyst suspension case. More effort needs to be devoted to improve the photocatalytic degradation of catalyst immobilized membrane. Also, the mechanical strength and durability of the materials remain as a challenge that inflicts the photodegradation performance and limit their wide scale application.

From energy point of view, utilization of renewable solar energy is attractive in water industry. Although several visible light induced photocatalysts have been developed [64-67], most of these photocatalytic membranes need to be initiated under UV irradiation. The effectiveness of catalysts within membrane matrix are jeopardized by the lower photocatalytic degradation and wide band gap energy. It is necessary to develop a novel catalyst that possesses small band gap energy, high surface area, and excellent resistance

against thermal shock. On the other hand, the transformation of organic pollutants might cause a variety of organic intermediates which can be toxic and more persistent than the original pollutants [68, 69]. Therefore, attentions also need to be paid to understand the adverse effects caused by the harmful by-products generated from the partial degradation of organic pollutants. Besides the targeted pollutants, the presence of inorganic impurities which cannot be degraded by photocatalytic membranes might accumulate on the membrane surface and unfavourably reduce the photocatalytic activity.

With respect to UV light, the key factor limiting the feasibility of the process at a real scale is the short life of the UV sources that must be periodically replaced. Additionally, operation of UV lamps consumes a lot of energy which was estimated to account for approximately 80% of the operation cost[70]. Although researchers have proposed to use ultraviolet light emitting diodes (UV-LED) that have longer life span and do not contain hazardous mercury, the purchase cost is still higher than UV lamps at same electrical energy conversion. Solar photocatalytic oxidation is a very promising process, however, it is limited by the large working area required for solar light irradiation. The research on the long term stability of novel photocatalyst with wavelength in the visible or solar light range is still insufficient.

In terms of safety, SMPR is needed to be properly covered to prevent direct exposure of UV light to human body. Proper cooling device is also required as high temperature might be incurred and causes overheating of the UV lamp in long run. In addition, the destructive effects of UV light or hydroxyl radicals on polymeric membranes is another key issue when photocatalysis is involved in the separation. It is because the immobilized photocatalysts might absorb UV light energy, causing membrane ageing and further altering its surface morphology and separation performance. It is in urgent need to find appropriate polymeric materials that are highly resistant towards UV irradiation and can be readily dissolved into a wide range of solvents.

4.0 Recommendations and Conclusion

The development of SMPR has undoubtedly contributed to the innovative and sustainable water treatment technologies. In this review article, the recent progress of SMPR are reviewed with respect to operating conditions during treatment process. The main intention of this contribution is to render the further insights into the impacts of each key operational parameter, i.e. catalyst loadings, light wavelength and intensity, feed concentration and pH, module packing density and ABFR on the performance of SMPR. The

understanding in this aspect is expected to provide a clue on the operating conditions that render optimum photocatalytic degradation efficiency for SMPR application. Numerous studies showed that the critical operational parameters might vary depending on the feed properties, catalyst type and the interaction between operating conditions. Therefore, the photocatalytic degradation of organic pollutants based on all the aforementioned parameters must be given due considerations.

Despite their assuring applications and significant achievement in recent decades, there are still some persistent problems that encountered in operating SMPR system. Some of them are reduced effectiveness of catalysts embedded within membrane matrix, polymer degradation under UV exposure and partial transformation of organic pollutants into hazardous by-products. The severe membrane fouling in the long term operation and its consequences on the plant maintenance and operating cost have limited the viability of SMPR in wastewater treatment industry. Gratefully, dedicated scientific investigations in recent years have offered several innovative approaches. For instances, the fabrication of dual layer hollow fiber membrane with catalyst immobilized into the outer surface layer. Dual-layer hollow fiber membranes have the advantages of maximizing membrane performance by using an extremely high-performance or functional membrane material as the selective layer while employing a low-cost material as the supporting layer. This approach reduces significantly the overall membrane material cost without compromising filtration and photocatalytic performance.

More research in this area is still required to resolve the aforementioned issues as well as to enhance the performance efficiency, reliability and stability of SMPR for industrial implementation. With the rapid progress made in material science and engineering, it is expected that newly developed catalysts can outperform the existing one under visible light or solar illumination. In terms of membrane materials, polymers that can withstand UV irradiation and can be easily dissolved in common solvents such as N-methyl-2-pyrrolidone and dimethylacetamide are highly desired. The use of ceramic membranes which possesses excellent thermal and chemical resistance and resists to abrasion by suspended photocatalysts may be another promising option. With respect to the system configuration, the photocatalytic membrane reactor design should be further improved based on the total irradiated surface area of catalyst per unit volume, the UV light power and its intensity as well as the light distribution within the reactor.

Last but not least, it is recommended to combine solar heterogeneous photocatalytic oxidation with photovoltaics to reduce the energy consumption of the process. In order to

reduce fouling problems in SMPR system, another photocatalyst removal pretreatment stage such as sedimentation or precoat filtration prior to membrane filtration might be advantageous, especially when solar photocatalytic oxidation is operated in batch mode. Although it might take years to resolve the remaining challenges in this field, it seems certain that SMPR will become more universal and effective in dealing with large variety of industrial wastewater application in the future.

References

1. *2014 Update: Progress on Drinking Water and Sanitation*, WHO/UNICEF Joint Monitoring Programme for Water Supply and Sanitation (JMP), 2014.
2. N. H. H. Hairom, A. W. Mohammad and A. A. H. Kadhum, *Separation and Purification Technology*, 2014, **137**, 74-81.
3. S. Mozia, D. Darowna, A. Orecki, R. Wróbel, K. Wilpiszewska and A. W. Morawski, *Journal of Membrane Science*, 2014, **470**, 356-368.
4. X. Li, X. Wu, G. He, J. Sun, W. Xiao and Y. Tan, *Chemical Engineering Journal*, 2014, **251**, 58-68.
5. G. Zhang, J. Zhang, L. Wang, Q. Meng and J. Wang, *Journal of Membrane Science*, 2012, **389**, 532-543.
6. F. Mohd Omar, H. Abdul Aziz and S. Stoll, *Science of The Total Environment*, 2014, **468–469**, 195-201.
7. L. M. Rossi, N. J. S. Costa, F. P. Silva and R. Wojcieszak, *Green Chemistry*, 2014, **16**, 2906-2933.
8. C. Luo, Q. Fu and C. Pan, *Scientific Report*, 2015, **5**.
9. K. Chikkadi, M. Mattmann, M. Muoth, L. Durrer and C. Hierold, *Microelectronic Engineering*, 2011, **88**, 2478-2480.
10. R. Molinari, L. Palmisano, E. Drioli and M. Schiavello, *Journal of Membrane Science*, 2002, **206**, 399-415.
11. M. N. Chong, B. Jin, C. W. K. Chow and C. Saint, *Water Research*, 2010, **44**, 2997-3027.
12. S. Mozia, *Separation and Purification Technology*, 2010, **73**, 71-91.
13. F. Gallucci, A. Basile and F. I. Hai, in *Membranes for Membrane Reactors*, John Wiley & Sons, Ltd, 2011, DOI: 10.1002/9780470977569.ch, pp. 1-61.
14. R. Molinari, P. Argurio and C. Lavorato, in *Membrane Reactors for Energy Applications and Basic Chemical Production*, eds. A. Basile, L. D. P. l. Hai and V. Piemonte, Woodhead Publishing, 2015, DOI: http://dx.doi.org/10.1016/B978-1-78242-223-5.00020-0, pp. 605-639.
15. R. Molinari, P. Argurio and L. Palmisano, in *Advances in Membrane Technologies for Water Treatment*, eds. A. Basile and A. C. K. Rastogi, Woodhead Publishing, Oxford, 2015, DOI: http://dx.doi.org/10.1016/B978-1-78242-121-4.00007-1, pp. 205-238.
16. R. Molinari, L. Palmisano, V. Loddo, S. Mozia and A. W. Morawski, in *Handbook of Membrane Reactors*, ed. A. Basile, Woodhead Publishing, 2013, vol. 2, pp. 808-845.
17. S. Mozia, A. W. Morawski, R. Molinari, L. Palmisano and V. Loddo, in *Handbook of Membrane Reactors*, ed. A. Basile, Woodhead Publishing, 2013, vol. 2, pp. 236-295.
18. J. Fu, M. Ji, Z. Wang, L. Jin and D. An, *Journal of Hazardous Materials*, 2006, **131**, 238-242.
19. S. S. Chin, T. M. Lim, K. Chiang and A. G. Fane, *Chemical Engineering Journal*, 2007, **130**, 53-63.
20. S. Ahmed, M. G. Rasul, W. N. Martens, R. Brown and M. A. Hashib, *Desalination*, 2010, **261**, 3-18.

21. D. P. Ho, S. Vigneswaran and H. H. Ngo, *Separation and Purification Technology*, 2009, **68**, 145-152.
22. Ö. Kerkez and İ. Boz, *Chemical Engineering Communications*, 2014, **202**, 534-541.
23. V. C. Sarasidis, K. V. Plakas, S. I. Patsios and A. J. Karabelas, *Chemical Engineering Journal*, 2014, **239**, 299-311.
24. C. Ong, W. Lau, P. Goh, B. Ng and A. Ismail, *Desalination*, 2014, **353**, 48-56.
25. R. A. Damodar and S.-J. You, *Separation and Purification Technology*, 2010, **71**, 44-49.
26. M.-J. Kim, K.-H. Choo and H.-S. Park, *Journal of Photochemistry and Photobiology A: Chemistry*, 2010, **216**, 215-220.
27. R. Halim, R. Utama, S. Cox and P. Le-Clech, *Membrane Water Treatment*, 2010, **1**, 283-296.
28. Y. Wei, H. Chu, B. Dong and X. Li, *Chin. Sci. Bull.*, 2011, **56**, 3437-3444.
29. V. C. Sarasidis, S. I. Patsios and A. J. Karabelas, *Separation and Purification Technology*, 2011, **80**, 73-80.
30. P. Wang, A. G. Fane and T.-T. Lim, *Chemical Engineering Journal*, 2013, **215–216**, 240-251.
31. X. Zhang, D. K. Wang, D. R. S. Lopez and J. C. Diniz da Costa, *Chemical Engineering Journal*, 2014, **236**, 314-322.
32. R. L. Fernández, J. A. McDonald, S. J. Khan and P. Le-Clech, *Separation and Purification Technology*, 2014, **127**, 131-139.
33. S. Kertèsz, J. Cakl and H. Jiránková, *Desalination*, 2014, **343**, 106-112.
34. C. S. Ong, W. J. Lau, P. S. Goh, B. C. Ng and A. F. Ismail, *Desalination*, 2014, **353**, 48-56.
35. S. Khan, J. Kim, A. Sotto and B. Van der Bruggen, *Journal of Industrial and Engineering Chemistry*, 2015, **21**, 779-786.
36. R. A. Damodar, S.-J. You and S.-H. Ou, *Separation and Purification Technology*, 2010, **76**, 64-71.
37. S. S. Chin, T. M. Lim, K. Chiang and A. G. Fane, *Desalination*, 2007, **202**, 253-261.
38. K.-H. Choo, R. Tao and M.-J. Kim, *Journal of Membrane Science*, 2008, **322**, 368-374.
39. Z. Ren, Y. Yang, W. Zhang, J. Liu and H. Wang, *Journal of Membrane Science*, 2013, **439**, 28-35.
40. M. Scholz, M. Wessling and J. Balster, in *Membrane Engineering for the Treatment of Gases: Volume 1: Gas-separation Problems with Membranes*, The Royal Society of Chemistry, 2011, vol. 1, pp. 125-149.
41. A. P. S. Yeo, A. W. K. Law and A. G. Fane, *Journal of Membrane Science*, 2006, **280**, 969-982.
42. J. Günther, P. Schmitz, C. Albasi and C. Lafforgue, *Journal of Membrane Science*, 2010, **348**, 277-286.
43. S. Chang and A. G. Fane, *Journal of Membrane Science*, 2001, **184**, 221-231.
44. J. Günther, D. Hobbs, C. Albasi, C. Lafforgue, A. Cockx and P. Schmitz, *Journal of Membrane Science*, 2012, **389**, 126-136.
45. S.-H. Yoon, H.-S. Kim and I.-T. Yeom, *Journal of Membrane Science*, 2004, **234**, 147-156.
46. W. Y. Kiat, K. Yamamoto and S. Ohgaki, *Water Science & Technology*, 1992, **26**, 1245-1254.
47. J. Wu and V. Chen, *Journal of Membrane Science*, 2000, **172**, 59-74.
48. T. Tasaki, T. Wada, K. Fujimoto, S. Kai, K. Ohe, T. Oshima, Y. Baba and M. Kukizaki, *Journal of Hazardous Materials*, 2009, **162**, 1103-1110.
49. PCO (Photo Catalytic Oxidation) Nano-Technology: How TiO2 UV Photocatalytic Oxidation (PCO) Works, http://www.air-oasis-uv-pco-sanitizers.com/how-pco-works.htm, (accessed 26th August 2015).
50. U. G. Akpan and B. H. Hameed, *Journal of Hazardous Materials*, 2009, **170**, 520-529.
51. R. M. Silverstein, G. C. Bassler and T. C. Morrill, *Spectrometric Identification of Organic Compounds 4th ed.* , New York: John Wiley and Sons, 1981.
52. W. Baran, A. Makowski and W. Wardas, *Dyes and Pigments*, 2008, **76**, 226-230.
53. S. Khan, J. Kim, A. Sotto and B. Van der Bruggen, *Journal of Industrial and Engineering Chemistry*, DOI: http://dx.doi.org/10.1016/j.jiec.2014.04.012.

54. N. Z. Searle, P. Giesecke, R. Kinmonth and R. C. Hirt, *Appl. Opt.*, 1964, **3**, 923-927.
55. A. Fujishima, T. N. Rao and D. A. Tryk, *Journal of Photochemistry and Photobiology C: Photochemistry Reviews*, 2000, **1**, 1-21.
56. T. Mano, S. Nishimoto, Y. Kameshima and M. Miyake, *Chemical Engineering Journal*, 2015, **264**, 221-229.
57. M. Miyauchi, A. Nakajima, T. Watanabe and K. Hashimoto, *Chemistry of Materials*, 2002, **14**, 2812-2816.
58. L. B. Khalil, W. E. Mourad and M. W. Rophael, *Applied Catalysis B: Environmental*, 1998, **17**, 267-273.
59. L. M. Pastrana-Martínez, S. Morales-Torres, V. Likodimos, J. L. Figueiredo, J. L. Faria, P. Falaras and A. M. T. Silva, *Applied Catalysis B: Environmental*, 2012, **123–124**, 241-256.
60. S. Mozia, D. Darowna, R. Wróbel and A. W. Morawski, *Journal of Membrane Science*, DOI: http://dx.doi.org/10.1016/j.memsci.2015.08.024, JMS15820.
61. S. S. Chin, K. Chiang and A. G. Fane, *Journal of Membrane Science*, 2006, **275**, 202-211.
62. R. Molinari, M. Mungari, E. Drioli, A. Di Paola, V. Loddo, L. Palmisano and M. Schiavello, *Catalysis Today*, 2000, **55**, 71-78.
63. J. Mendret, M. Hatat-Fraile, M. Rivallin and S. Brosillon, *Separation and Purification Technology*, 2013, **118**, 406-414.
64. C. P. Athanasekou, S. Morales-Torres, V. Likodimos, G. E. Romanos, L. M. Pastrana-Martinez, P. Falaras, D. D. Dionysiou, J. L. Faria, J. L. Figueiredo and A. M. T. Silva, *Applied Catalysis B: Environmental*, 2014, **158–159**, 361-372.
65. N. Raghavan, S. Thangavel and G. Venugopal, *Materials Science in Semiconductor Processing*, 2015, **30**, 321-329.
66. P. Fernández-Ibáñez, M. I. Polo-López, S. Malato, S. Wadhwa, J. W. J. Hamilton, P. S. M. Dunlop, R. D'Sa, E. Magee, K. O'Shea, D. D. Dionysiou and J. A. Byrne, *Chemical Engineering Journal*, 2015, **261**, 36-44.
67. Y. Zhang, N. Zhang, Z.-R. Tang and Y.-J. Xu, *ACS Nano*, 2012, **6**, 9777-9789.
68. S. Parra, V. Sarria, S. Malato, P. Péringer and C. Pulgarin, *Applied Catalysis B: Environmental*, 2000, **27**, 153-168.
69. A. Bianco Prevot, M. Vincenti, A. Bianciotto and E. Pramauro, *Applied Catalysis B: Environmental*, 1999, **22**, 149-158.
70. H. Gulyas, *Journal of Advanced Chemical Engineering*, 2014, **4**, 108.